10R.1

DUAL-POLARIZATION OBSERVATIONS OF TORNADOES AT CLOSE RANGE MADE WITH A MOBILE X-BAND DOPPLER RADAR

Howard B. Bluestein*, and Michael M. French
University of Oklahoma
Norman, Oklahoma

Stephen Frasier, Kery Hardwick, Francesc Junyent, and Andrew L. Pazmany[1]
University of Massachusetts
Amherst, Massachusetts

1. INTRODUCTION

Polarimetric radar data have been used to discriminate among the various types of scatterers in the atmosphere. Ryzhkov et al. (2005) were the first to collect polarimetric data in tornadoes and discriminate between debris and hydrometeors. Using a prototype of the polarimetric NEXRAD, they found in three cases that tornado debris signatures were characterized by relatively low differential reflectivity (Z_{DR}) and low cross-correlation coefficient (ρ_{HV}). They interpreted their results in the light of the numerical simulations of scatterers in tornado-like vortices (Dowell et al. 2005). In particular, they suggested that the low values of differential reflectivity were associated with lofted light debris; higher values of differential reflectivity, which were associated with hydrometeors, were found at greater distances from the center of the tornadoes.

In this study, we examine additional data collected with a polarimetric Doppler radar in three tornadoes in the spring of 2004. The data collected differ from the data discussed by Ryzhkov et al. (2005). First, the radar was located much closer to the tornadoes, so that the spatial resolution was much higher. In fact, in two of the cases the tornado and its debris cloud were visible, so that photogrammetric analysis of the dimensions of the debris cloud was possible for comparison with the radar data. Secondly, the data were collected by an X-band radar, rather than by an S-band radar. Finally, data were collected only at one elevation angle, not in a volume.

2. DATA COLLECTION AND PROCESSING

Data were collected by a mobile, X-band, polarimetric Doppler radar designed and built at the Microwave Remote Sensing Laboratory (MIRSL) at the Univ. of Massachusetts in Amherst. A more detailed description of the radar and its capabilities is found in Pazmany et al. (2003), Lopez et al. (2004), and Kramar et al. (2005).

The truck-mounted radar uses a parabolic dish antenna having a half-power beamwidth of 1.25 deg. The radar system was built from an inexpensive, marine radar. The data processing system in 2004 allowed for two modes of data collection: (a) "surveillance" mode and (b) "data-collection mode". In the former, only radar reflectivity was computed and recorded. In the latter, Doppler velocity and differential reflectivity and differential phase (ϕ_{DP}) were also computed, and recorded out to 30 km range. The processing was done later at MIRSL and made available in a format compatible for use with SOLO (Oye 1995). The Doppler velocity data, which folded at ±18 m s^{-1}, were easily unfolded. The real-time display functioned for reflectivity only and only when the radar was in "surveillance" mode.

Scans were done at an elevation angle as close to the ground as possible, yet above most intervening trees, buildings, etc. Field operations were conducted as in past years (Kramar 2005).

3. CASE STUDIES

a. Tornadoes on 12 May 2004 in southern Kansas

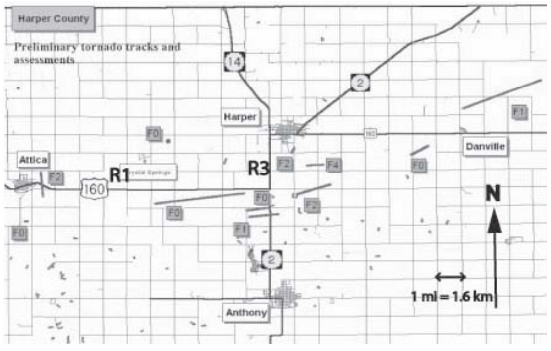

Figure 1. Tornado tracks and estimated F-scale rating of each tornado on 12 May 2004, as determined by the National Weather Service, Wichita, KS. Also shown are two of the deployment sites (R1 and R3) of the U. Mass. mobile, X-band radar when data were being collected, for the second and fourth tornado.

* *Corresponding author address:* Howard B. Bluestein, School of Meteorology, Univ. of Oklahoma,Norman,OK 73019; e-mail: hblue@ou.edu

[2]Current affiliation: ProSensing, Inc., Amherst, MA

A series of tornadoes in a supercell formed in south-central Kansas on 12 May 2004 (Fig. 1). The first tornado in which data were successfully collected (Fig. 2) tracked approximately northward, or north-northwestward near Attica, KS; the location of the radar was at R1, approximately 3 – 4 km from the tornado.

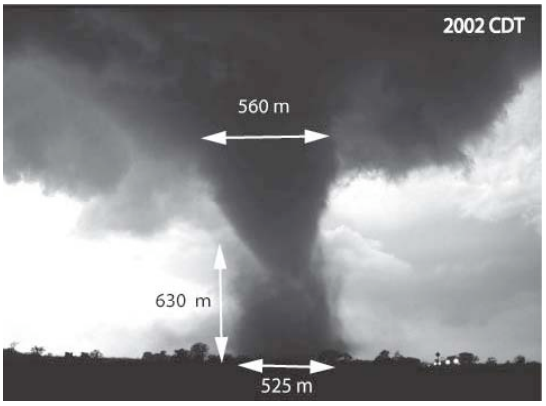

Figure 2. Photograph of a tornado, during its mature stage, on 12 May 2004, at 2002 CDT. The view is to the west from a location approximately 5 km east of Attica, KS. Photograph copyright H. Bluestein. The approximate dimensions of the opaque debris cloud, condensation funnel, and height of the cloud base, as determined from photogrammetric analysis, are as indicated.

The radar imagery of the tornado generally was characterized by a ring of more intense reflectivity surrounding a weak-echo "eye," which in turn was surrounded by one or more spiral bands (Fig. 3a). Such features are common in tornadoes (Dowell et al. 2005). The tornado was marked by relatively low values of differential reflectivity or near zero Z_{DR} (Fig. 3b). The circular area of low Z_{DR} was approximately 900 m in diameter, which was about twice the width of the circular debris cloud under the condensation funnel, but approximately the same as the width of the entire debris cloud (Fig. 2). The shape of the region of low Z_{DR} changed rapidly from scan to scan (not shown), as did the visual appearance of the debris cloud. The low-Z_{DR} region was collocated within an area that contained relatively high reflectivity in the ring. The Doppler velocity couplet associated with the tornado was not very intense (Fig. 3c), even though the tornado was rated at F2 intensity. The maximum Doppler velocity was only around 25 m s^{-1}. It is likely that the radar beam was not low enough to sample the highest wind speeds, owing to the intervening trees on the horizon.

The third tornado in which data were successfully collected (Fig. 4) tracked to the east-northeast. Even though this tornado had a large debris cloud, the damage was rated only F0. The

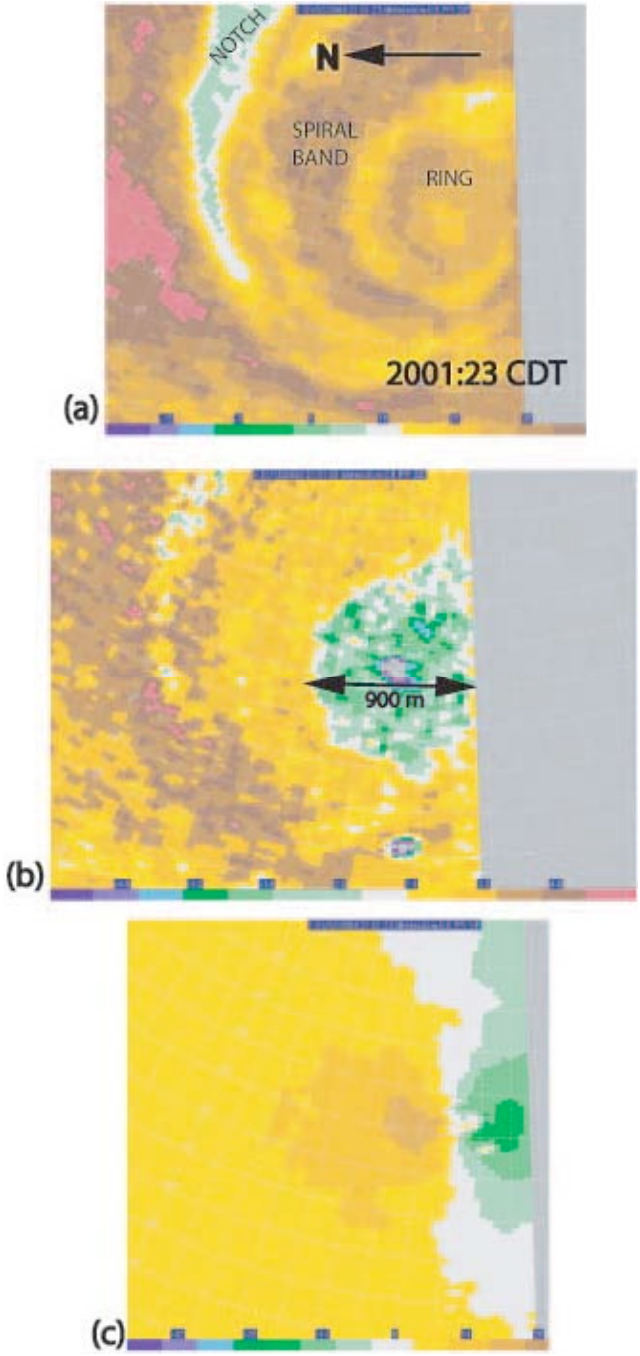

Figure 3. Features of the second tornado on 12 May 2004, as depicted by small-scale data collected by the U. Mass., mobile, X-band, Doppler radar, at low elevation angle. (a) radar reflectivity factor (dBZ), (b) differential reflectivity, Z_{DR} (dBZ), and (c) Doppler velocity (m s^{-1}) at 2001:23 CDT. Range markers are displayed every 250 m; range marker values are given in km, but are truncated/rounded (so, e. g., 4.2 km is actually 4.25 km and 4.8 km is actually 4.75 km). Color codes for the scale of the parameters shown in each panel are shown at the bottom of each panel.

radar was around 3 – 4 km from the tornado (R3 in Fig. 1).

Figure 4. Image of the tornado subsequent and to the east of the Attica, KS tornado (the fourth tornado) at approximately 2022 CDT. Image is from a frame captured by a video, copyright H. Bluestein. View is to the southwest. (cf. Fig. 1).

The radar imagery from this tornado (Fig. 5) displayed similar characteristics to those evident in Fig. 3. In this case, however, in addition to a region of relatively low values of Z_{DR} (Fig. 5b) around the weak-echo "eye" (Fig. 5a), which marked the center of the tornado (Fig. 5c), there was also a broken ring of low values of Z_{DR} surrounding the eye, which was collocated with a region of higher reflectivity.

b. Tornadoes on 29 May 2004 in central Oklahoma

A high-precipitation (HP) supercell (Doswell et al. 1990) in central Oklahoma on 29 May 2004 spawned several tornadoes. Data were collected in a few of these tornadoes from a vantage point near Calumet, OK (Fig. 6). Unlike the tornadoes on 12 May 2004, the tornadoes on 29 May were either hidden from view by heavy precipitation or were not easily seen because the contrast was poor (Fig. 7). Viewed from the east, the cloud base was laminar, striated, and flared. To the right (north) of the cloud base there was a relatively bright region.

The main body of the radar echo associated with the storm (Fig. 8) was connected to a relatively narrow band to a region, collocated with the cloud base seen in Fig. 7a (determined by photgrammetric analysis); behind an arc of intense precipitation there was a weak-echo "eye." The notch in relatively low reflectivity to the right (east) of the eye was collocated with the relatively bright region seen in Fig. 7a. It is clear why any tornado collocated with the eye would not have been visible to an observer located to the east.

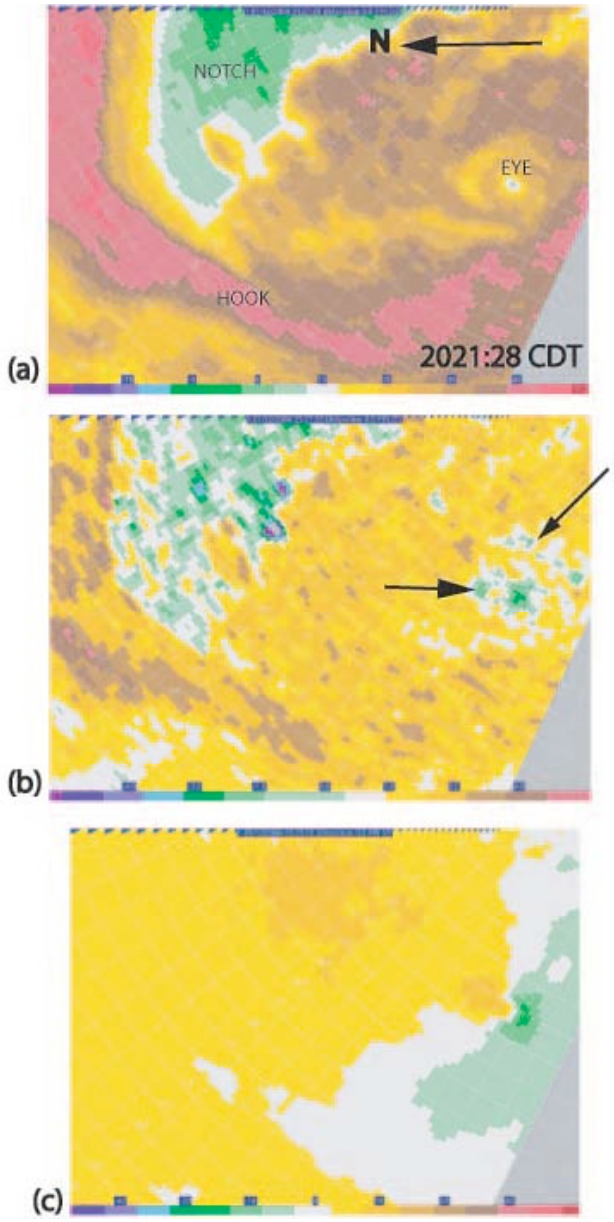

Figure 5. As in Fig. 3, but for the tornado seen in Fig. 4, at 2021:28 CDT; the range markers are given in km and spaced every 200 m. Arrows in (b) point to regions of relatively low values of Z_{DR} surrounding the eye of the tornado, in regions of relatively high radar reflectivity.

The appearance of the eye changed from scan to scan (Figs. 9 and 10). In general, the eye was much wider than that of the eyes on 12 May 2004 discussed earlier; the eye in the 29 May tornado depicted in Figs. 8, 9a and 10a was approximately 1.5 km in diameter, while the eye in the 12 May 2004 tornadoes, whose central reflectivity was not

Figure 6. Approximate tornado tracks of two tornadoes on 29 May 2004, as determined by the National Weather Service, Norman, OK (courtesy Rick Smith, Warning Coordination Meteorologist). Also shown are the deployment sites (R1 and R2) of the U. Mass., mobile, X-band radar. Base map courtesy Mapquest. Approximate times are given along the tracks in CDT. The second track was for a rare, anticyclonic tornado. Damage in the first track was rated as F1, almost F2.

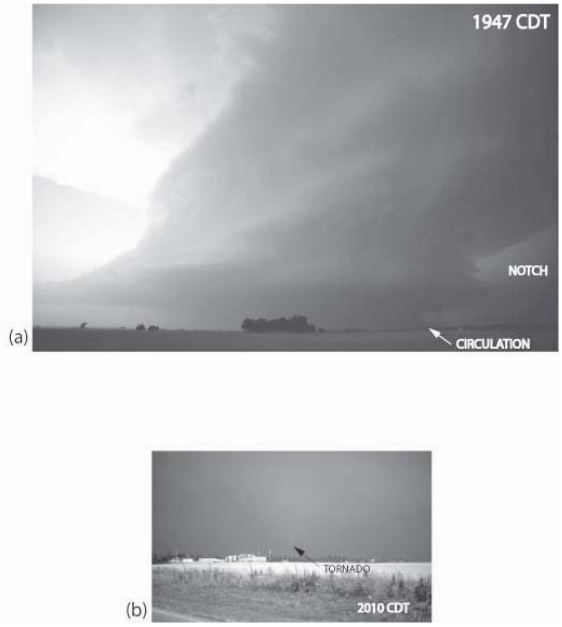

Figure 7. Images of (a) the supercell near Geary, OK, on 29 May 2004, viewed from the east, 1.6 km north of Calumet, OK, at ~1947 CDT; wide-angle view is to the west and (b) one of the tornadoes (reported to be anticyclonic) spawned to the east/northeast of Calumet, at 2010 CDT, viewed to the northeast from 1.1 km south of Calumet (cf. Fig. 6). Any tornado present in the storm when (a) was taken would have been in the lower right-hand sector of the image (denoted by "circulation"), hidden by precipitation. Photographs copyright H. Bluestein.

weak, was approximately only 150 – 200 m in diameter.

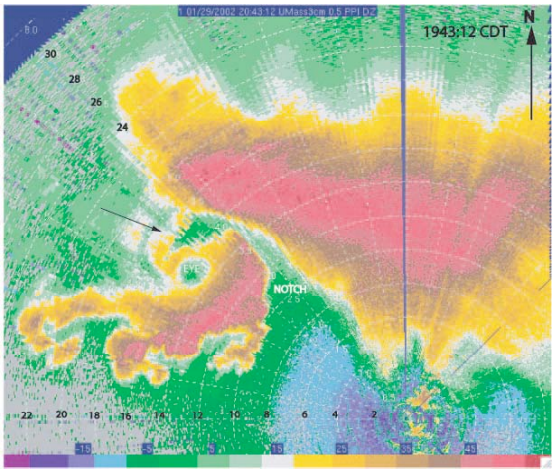

Figure 8. Storm-scale depiction of the radar reflectivity (dBZ) in the Geary/Calumet supercell on 29 May 2004, at 1943:12 CDT. Data were collected by the U. Mass. X-band radar in "surveillance mode" (without corresponding Doppler velocity and differential reflectivity data). Range markings are given (in black) in km, every 2 km; the white range markers are given in km/4. The arrow points to a band of reflectivity that connects the main body of the storm to the "eye" and rear-flank gust front in the lower-left quadrant of the image. The "notch" of low reflectivity corresponds to the bright area seen in the lower right portion of Fig. 7a. The lack of data in a narrow swath to the north of the radar is due to beam blockage.

The differential reflectivity on the left side (to the west and northwest) of the center of the tornado eye (Figs. 9b and 10b) was relatively low, even though the reflectivity was not relatively low (Figs. 9a and 10a). At 1950:07 CDT there was a narrow appendage within the eye, of relatively high reflectivity and differential reflectivity. It is suggested that this appendage represents hydrpmeteors being drawn into the center of the 1.5-km scale tornado vortex by the circulation of the tornado (Fig. 10c). So, in contrast to the 12 May 2004 tornadoes, there was no debris signature encircling the tornado; however, there was a debris signature to the west of the tornado circulation. As in the 12 May tornadoes, the maximum Doppler velocities appeared to be weaker (~ 28 m s^{-1}) than what would be expected in a tornado. As in that case, it is likely that the radar beam was above the level of the maximum wind speeds.

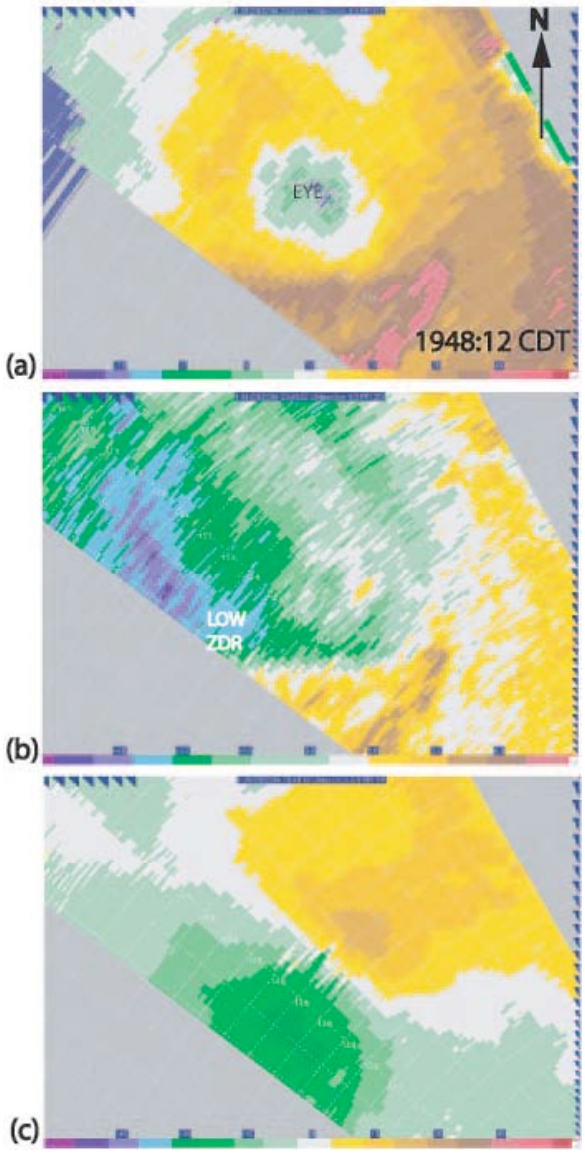

Figure 9. As in Fig. 3, but for a tornado northwest of Calumet, OK, on 29 May 2004, at 1948:12 CDT and with range markers shown at 500 m range increments.

While the parent supercell propagated to the east and northeast, the radar team cautiously retreated to the south. A tornado formed to the northeast of the location of the radar (Figs. 6 and 7b). This tornado, which was reported to be anticyclonic, was associated with a hook echo (Fig. 11) just before it formed, that was the mirror-image of the hook echoes associated with cyclonic vortices. The remnants of the older, cyclonic tornado depicted by radar in Figs. 8 – 10 was still associated with a weak-echo eye. The anticyclonic hook was positioned about 10 km to the southeast of the weak-echo eye associated with the cyclonic

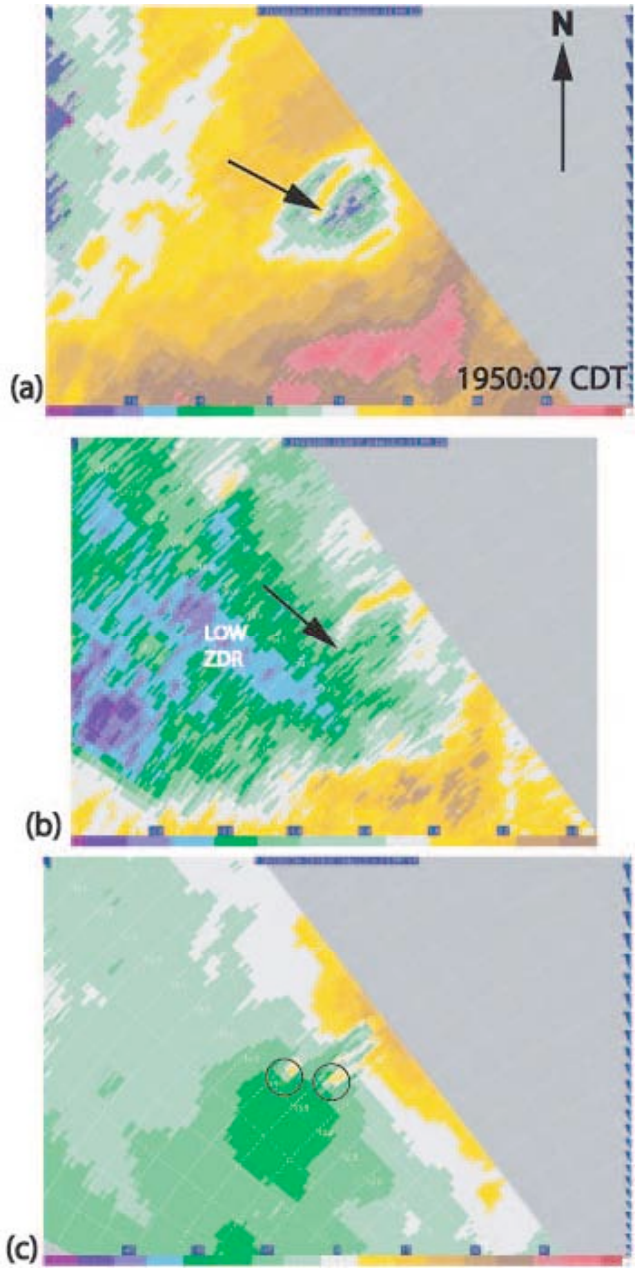

Figure. 10. As in Fig. 9, but at 1950:07 CDT. Multiple-vortex signatures are evident in this scan (indicated by circles in c). However, the automatic unfolding algorithm may have failed near the data-sparse region of the eye; manual unfolding did not unambiguously support the existence of the multiple vortices. The arrows in (a) and (b) point to an appendage within the eye of relatively high radar reflectivity and relatively high differential reflectivity, respectively.

tornado. It appears as though the anticyclonic hook was located at the southern end of the radar-echo segment associated with the rear-flank gust front, while the cyclonic tornado was located at the northern end. Such a configuration

has been observed on the rare occasions when a pair of cyclonic and anticyclonic tornadoes have been documented in supercells (Brown and Knupp 1980; Fujita 1981).

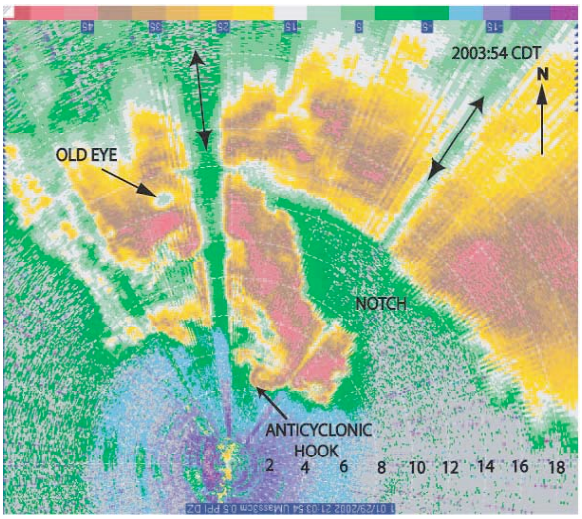

Figure 11. As in Fig. 8, but at 2003:54 CDT. A rare, anticyclonic hook echo is noted. Two swaths of significant beam blockage are indicated by the line segments with double arrows.

No significant signature in the field of differential reflectivity is evident in the old eye (Fig. 12). Unfortunately, neither Doppler data nor differential reflectivity data were available in the sector containing the anticyclonic tornado, owing to a processing problem.

4. SUMMARY AND CONCLUSIONS

Data collected at close range by a mobile, polarimetric, X-band, Doppler radar in several tornadoes had characteristics similar to the data collected by Ryzhkov et al. (2005) from a fixed-site, polarimetric, S-band Doppler radar: For some times tornadoes were collocated with a quasi-circular area of relatively low values of Z_{DR}, which is thought to represent the debris lofted. In one well-documented case (12 May 2004), it was found from photograpmmetric analysis of a photograph of the tornado probed by radar that the visible debris cloud was of approximately the same width as the region of low values of Z_{DR}. In another case (29 May 2004), the tornado was apparently embedded within precipitation in an HP supercell and therefore not visible. It was therefore not possible to determine whether or not there was a debris cloud in this tornado. However, there was a swath of relatively low values of Z_{DR} on one side of the tornado, not collocated with high reflectivity, that may have been associated with a band of debris just above the ground.

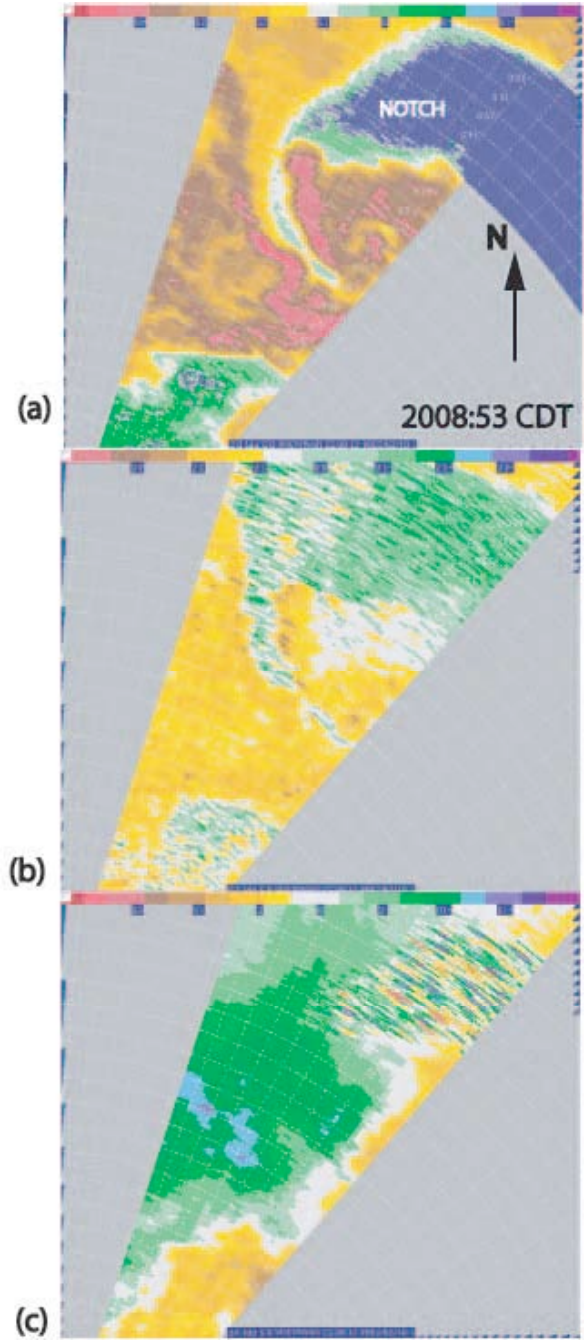

Figure 12. As in Fig. 9, but at 2008:53 CDT. The remnants of the cyclonic circulation seen with the eye in Figs. 8 - 11 are evident to the south of the echo “notch,” to the northeast of the radar about 12 km in range. Doppler data in the anticyclonic hook area seen in Fig. 11 are not available, owing to processing problems. Cf. Fig. 7b for a view of the tornado just a minute later.

It is clear that polarimetric Doppler radars have the capability to distinguish airborne debris lofted by tornadoes from hydrometeors. The high-resolution reflectivity, differential reflectivity, and Doppler velocity collected by the U. Mass. X-band radar represented only selected times at one elevation angle. It is hoped that in the future data will be collected in tornadoes at the same spatial scales, but at shorter temporal scales and for full volume scans that cover the depth of the tornado and features within the parent storm.

ACKNOWLEDGMENTS

This research was funded by NSF grants ATM-ATM-0241037 to OU and ATM-0000592 to U. Mass. Support was also provided by the School of Meteorology at the University of Oklahoma (OU). The second author operated the radar in the field. The authors thank Mark Laufersweiler (OU) for his assistance with computer-related issues. Rick Smith at the NWS in Norman provided damage survey information for the 29 May storm.

REFERENCES

Brown, J. M. and K. R. Knupp, 1980: The Iowa cyclonic-anticyclonic tornado pair and its parent thunderstorm. *Mon. Wea. Rev.,* **108**, 1626 - 1646.

Doswell, C. A., A. R. Moller, and R. Przyblinski, 1990: A unified set of conceptual models for variations on the supercell theme. Preprints, *16th Conf. on Severe Local Storms,* Kananaskis Park, AB, Canada, Amer. Meteor. Soc., 40 – 45.

Dowell, D. C., C. R. Alexander, J. M. Wurman, and L. J. Wicker, 2005: Reflectivity patterns and wind-measurement errors in high-resolution radar observations of tornadoes. *Mon. Wea. Rev.* , **133**, 1501 – 1524.

Fujita, T. T., 1981: Tornadoes and downbursts in the context of generalized planetary scales. *J. Atmos. Sci.*, **38**, 1511 - 1534.

Kramar, M. R., H. B. Bluestein, A. L. Pazmany, and J. D. Tuttle, 2005: The "Owl Horn" radar signature in developing Southern Plains supercells. *Mon. Wea. Rev.*, **133**, 2608 – 2634.

Lopez, F. J., A. L. Pazmany, H. B. Bluestein, M. R. Kramar, M. M. French, C. C. Wess, and S. Frasier, 2004: Dual-polarization, X-band, mobile Doppler radar observations of hook echoes in supercells. Preprints, *22nd Conf. on Severe Local Storms*, Hyannis, MA, Amer. Meteor. Soc., Amer. Meteor. Soc., CD-ROM, P11.7.

Oye, R., C. K. Mueller, and S. Smith, 1995: Software for radar translation, visualization, editing, and interpolation. *Preprints, 27th Conf. on Radar Meteorology*, Vail, CO, Amer. Meteor. Soc., 359-361.

Pazmany, A. L., F. J. Lopez, H. B. Bluestein, and M. Kramar, 2003: Quantitative rain measurements with a mobile, X-band, polarimetric Doppler radar. Preprints, *31st Conf. on Radar Meteor.*, Seattle, WA, Amer. Meteor. Soc., 858 – 859.

Ryzhkov, A. V., T. J. Schuur, D. W. Burgess, and D. S. Zrnic, 2005: Polarimetric tornado detection. *J. Appl. Meteor.*, **44**, 557 – 570.